Sol-Gel Coatings for Chemical Protection of Stainless Steel

Code: EP7

PEDRO DE LIMA NETO, MOHAMED ATIK, LUIS A. AVACA AND MICHEL A. AEGERTER

Institute of Physics and Chemistry of São Carlos, University of São Paulo, Cx. Postal 369 – 13560-970 – São Carlos (SP), Brazil

Abstract. Sol-gel thin coatings of ZrO_2, SiO_2, $70SiO_2-30TiO_2$ and $88SiO_2-12Al_2O_3$ compositions (mole %) have been prepared from sonocatalyzed sols and deposited by dip-coating technique on 316L stainless steel foils. The influence of the coatings on the chemical corrosion of the substrate has been measured through potentiodynamic polarization curves in aqueous 15% H_2SO_4 solution between 25 and 50°C. The values of the corrosion potential, polarization resistance and corrosion rate have been determined. Analysis of the data combined with scanning electron microscopy studies indicate that the films act as a geometric blocking against exposure to the corrosive media and increase the lifetime of the substrate up to a factor 8.5.

Keywords: thin film, ZrO_2, SiO_2, SiO_2-TiO_2, $SiO_2-Al_2O_3$, corrosion protection, stainless steel 316L

1. Introduction

Sol-gel methods are now widely used for the preparation of films of oxide materials from solutions and offer potential advantages over traditional techniques [1] [2] [3] [4]. The chemical processing [5] and the technical applications [6], which encompass optical,electronic, optoelectronic, photonic, biotechnology, chemical and mechanical fields have been reviewed recently.

Inorganic coatings having a vitreous structure are widely used as protective coatings for metals and alloys [7] [8]. They improve the chemical and physical properties of the metal surfaces relative to corrosion, friction and wear without altering the original properties of strength and toughness of the substrate.

The preparation and characterization of sol-gel films having these specific chemical and mechanical functions have been so far scarcely studied. Al_2O_3 [9], Si–O–N, Si_3N_4 [10] [11] films have been proposed for semiconductor passivation. SiO_2 [12] and TiO_2-SiO_2 [13] are known to prevent alkali diffusion. The prevention of chemical corrosion and oxidation of mild steel, carbon steel and stainless steels has been tested with SiO_2 [14], $SiO_2-B_2O_3$ [15] [16], mullite [17], ZrO_2 [15, 18–22], MTOS [23] and ZrO_2-CeO_2 [24] coatings. They all increase the protection of metal substrates from air corrosion (tested up to 800°C) and acid attack (tested up to 80°C).The most promising

prevention for stainless steel has been so far reported by our group using sol-gel film of ZrO_2, SiO_2-TiO_2, $SiO_2-Al_2O_3$ and TiO_2-CeO_2 prepared by dip-coating using sonocatalyzed sols [18, 19, 21, 25].

In this paper we present the results of a systematic electrochemical corrosion study in 15% aqueous H_2SO_4 up to 50°C of sol-gel films of ZrO_2, SiO_2-TiO_2, $SiO_2-Al_2O_3$ (mole%) deposited on stainless steel 316L by dip coating, a material widely used for marine and chemical industry environments.

2. Experimental

316L stainless steel substrates (Caseurop, France) were cut from large foils and degreased ultrasonically in acetone. This austenitic material was chosen because it has a low carbon content (<0.03%) and is therefore less susceptible to sensitization during the heat treatment necessary for the densification of the coatings.

The zirconia sol was prepared by dissolving the alkoxide $Zr(OC_3H_7)_4$ in isopropanol (C_3H_7OH) with a small amount of acetic acid (CH_3COOH). Excess water was then added to complete the hydrolysis. The concentration of the alkoxide was varied between 0.025 and 0.9 mole/1 ZrO_2. The volume ratios H_2O/C_3H_7OH and H_2O/CH_3COOH were respectively equal to 1 and 2. The silica sol was prepared by dissolving tetraethylorthosilicate $Si(OC_2H_5)_4$ in absolute
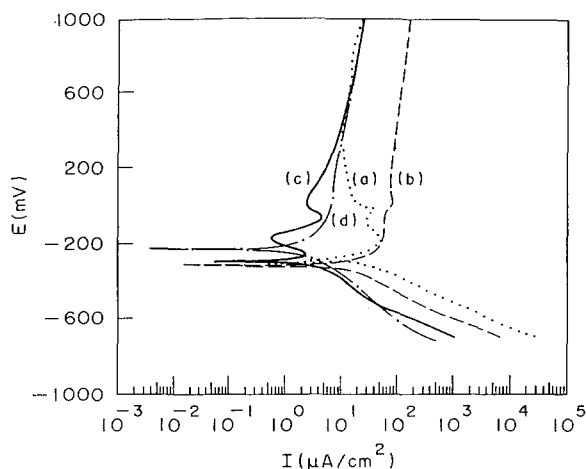
Fig. 1. Potentiodynamic polarization curves measured in deareated 15% aqueous H_2SO_4 at 25°C for 316L stainless steel a) uncoated and untreated, b) uncoated but heat treated at 800°C for 2 h., c) coated with ZrO_2 (800°C/2 h), d) coated with SiO_2 (800°C/2 h).

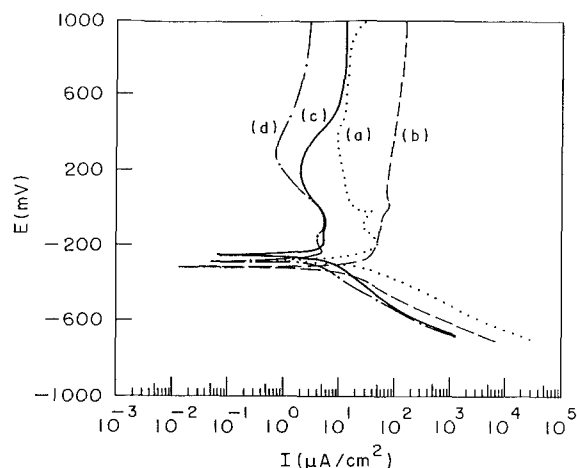*Fig. 2.* Same as figure 1 for T= 25°C a) and b) same as in Figure 1 (for reference); c) coated with SiO_2–TiO_2 (800°C/2 h); d) coated with SiO_2–Al_2O_3(800°C/2 h).

ethanol C_2H_5OH (0.43 mole/mole of alkoxide) to which a small amount of acetic acid CH_3OOH (0.087 mole/mole of alkoxide) was added. Binary compositions in the system SiO_2–TiO_2 and SiO_2–Al_2O_3 have been prepared using the same protocol and concentration using $Si(OC_2H_5)_4$, tetraorthotitanate $Ti(OC_2H_5)_4$ and aluminum sec-butilate $Al(OC_4H_5)_3$ as source of Si, Ti and Al respectively. The composition of the solutions were $xSiO_2(1-x)M_yO_z$ where M = Ti or Al with $x = 70$ mole% ($70SiO_2$–$30TiO_2$) and $x = 88$ mole% ($88SiO_2$–$12Al_2O_3$). However a complete study with $0 < x < 100$ for both binary systems is underway and will be published elsewhere. All the sols were submitted to intense ultrasonic irradiation (Heat Systems Ultrasonics W385). They became homogeneous and transparent after 25 minutes and were stable up to 4 weeks at room temperature when kept in a close vessel.

Single layer coatings have been deposited by dip coating technique at a constant withdrawal speed of 10 cm min^{-1}, dried at 60°C for 15 min. and then treated in air at a slow rate of 5°C min^{-1} up to 800°C, with an intermediate isothermal holding at 450°C during 1 h and further isothermal treatments at 800°C up to 20 h. The coatings have a thickness of about 0.3 to 0.6 μm. 1° glancing incidence X-ray diffraction (Rigaku Rotaflex) shows that the heat treated SiO_2 and $88SiO_2$–$12Al_2O_3$ coatings are amorphous; however ZrO_2 coatings crystallized at ~450°C into a tetragonal structure [21] while $70SiO_2$–$30TiO_2$ coatings partially

crystallized at ~650°C showing anatase crystallites in an amorphous silica matrix [21].

Electrochemical measurements are convenient and precise methods to evaluate the corrosion of a material in a given medium [26]. They have been carried out with freshly prepared samples in deareated 15% H_2SO_4 (Merck p.a.) aqueous solutions (Milli-Q) up to 50°C using a computerized PAR 273 Potentiostat/Galvanostat. A saturated calomel electrode (SCE) was used as reference and a Pt foil served as the auxiliary electrode. The working electrodes were immersed 1 cm into the solution. The potentiodynamic measurements were initiated at −0.7 V and scanned continuously toward the anodic direction at 1 mV s^{-1}. The data were analyzed with the PAR 342 Corrosion Measurement Software. A detailed explanation of the procedure and analysis of the results can be found in [25].

3. Results and Discussion

Potentiodynamic polarization curves have been measured at 25, 40 and 50°C. Figures 1 and 2 show typical results obtained at 25°C for stainless steel (ss) without coating and untreated, ss without coating but heat treated at 800°C during 2 h, ss with ZrO_2 coating (800°C/2 h), ss with SiO_2 coating (800°C/2 h), ss with SiO_2–Al_2O_3 coating (800°C/2 h), and ss with SiO_2–TiO_2 coating (800°C/2 h). Similar data have been obtained at the other temperatures.

The protective effect is noticeable for all coatings in both the cathodic and anodic branches of the

Table 1. Corrosion parameters determined from the potentiodynamic curves measured for stainless steel 316L (ss) uncoated and untreated, uncoated but heat treated at 800°C/2 h, coated with ZrO_2, SiO_2, $SiO_2-Al_2O_3$, and SiO_2-TiO_2 (800°C/2 h): corrosion potential E_{corr} (mV); polarization resistance R_p (kΩ cm^2) and corrosion rate CR (mills per year, MPY).

Sample	$T(°C)$	$-E_{corr}$ (mV)	R_p (kΩ cm^2)	CR (MPY)
SS 316L	25	286	1.80	11.5
untreated	40	261	0.37	35.2
	50	280	0.35	53.8
SS 316L heat	25	306	1.45	5.0
treated	40	304	0.57	19.8
	50	307	0.14	41.2
SS + ZrO_2	25	308	10.50	3.4
	40	328	8.50	4.2
	50	299	0.99	12.9
SS + SiO_2	25	289	8.56	3.1
	40	307	1.21	6.5
	50	314	0.31	14.2
SS + 88SiO_2–	25	240	5.92	4.2
12Al_2O_3	40	297	0.93	8.4
	50	301	0.89	13.9
SS + 70SiO_2–	25	291	10.7	2.2
30TiO_2	40	297	5.70	5.7
	50	293	3.10	6.3

curves. The cathodic part corresponds to the hydrogen evolution reaction $2H^+ + 2e^- \rightarrow H_2$. The slope of the curves for uncoated and untreated stainless steel is ca. 2.3 × 2 RT/F, where R is the universal gas constant and F the Faraday constant a value coherent with a Volmer–Heyrovsky sequence, a current mechanism accepted for this reaction [27]. In the presence of the coatings, the value of the slope is maintained suggesting that the mechanism remains unchanged. However there is a downward shift in the current densities (in the sequence: untreated ss, heat treated ss, $SiO_2-Al_2O_3$, SiO_2-TiO_2, ZrO_2) indicating that the films act as a geometric blocking; they act as an inert obstacle to exposure of the metal surface to its environment and therefore the reaction rates fall in proportion to the extent of surface coverage. As an example the active area for the reaction is typically reduced by a factor of 10 for the best coating (SiO_2TiO_2). The chemical attack is probably done via a small remaining open porosity of the film (not observed in SEM measurements) left after the densification heat treatment. The position and the slope of the SiO_2-TiO_2 potentiodynamic curves measured in the cathodic range at 25°C do not change for heat treatment up to 15 h, all being identical to curve d of Figure 2 indicating that the film surface

coverage is not affected by these heat treatments. The measurements performed at 40°C and 50°C present similar behavior and consequently the blocking properties remain unchanged at these temperatures.

An intermediate behavior is observed for the heat treated substrates without coating (curves b of Figures 1 and 2). It is difficult to interpret it without a detailed knowledge of the processes occurring in the oxide layers growing during the heat treatment on the stainless steel surface as well as in its bulk structure.

The anodic branches of the polarization curves show that the coatings have a strong effect on the current density in the passive region, diminishing the current value of uncoated and untreated stainless steel by roughly one order of magnitude. In the same region, the heat treated uncoated ss samples (curve b of the Figures 1 and 2) show current densities somewhat higher than those of the untreated substrates (curve a) revealing again surface changes during the treatment.

The combined cathodic and anodic effects of the coatings on the corrosion behavior of 316L stainless steel are summarized in Table 1, which presents the relevant corrosion parameters derived from computer analysis of the potentiodynamic curves. The values of
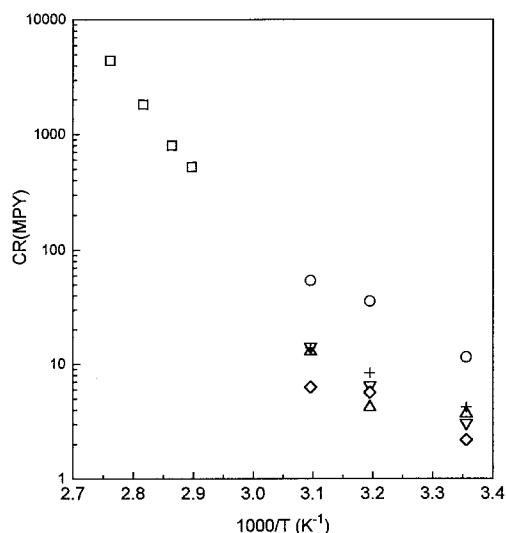
Fig. 3. Temperature dependence of the corrosion rate (MPY) in deareated 15% aqueous H_2SO_4 solution of 316L stainless steel: ($\square$, $\circ$) uncoated and untreated; the high temperature data ($\square$) are from [19] and have been obtained by weight loss in non deareated solution; (∇) coated with SiO_2; ($\triangle$) ZrO_2; ($+$) SiO_2–Al_2O_3 and ($\diamond$) SiO_2–TiO_2.

the corrosion potential (E_{corr}) are very little affected by the presence of the films indicating a balance between cathodic and anodic effects. However the polarization resistances (R_p) which reflects the kinetics of the process at the equilibrium potential and the corrosion rate (CR), measured in mill per year, are drastically changed. At all tested temperatures all coatings show a lower corrosion rate than the untreated and uncoated substrate. The lifetime of the coated substrates is increased typically by a factor 3,5 to 5,5 at 25°C. The effect is even more pronounced at 40°C (4 to 8) and reaches 8.5 for SiO_2–TiO_2 at 50°C but decreases to 4 for the other coatings. Even in relation to the heat–treated uncoated ss samples, which appear to be more acid resistant than the untreated samples, the effect of the coating is still considerable.

The corrosion rates determined for the different coating compositions heat treated at 800°C for 2 h. increase with the temperature of the electrolyte (Figure 3). The low temperature data show the same overall Arrhenius behavior (activation energy $E = 27$–28 kcal mole $^{-1}$) for all coatings as well as for the uncoated stainless steel. For the oxide coatings however the preexponential factor is smaller. This confirms that the layers act as a geometric blocking. The data at high temperatures have been determined by weight loss measurements in non deareated H_2SO_4 solution

[19]. In order to truly compare these values to those determined electrochemically the measurements should have been extrapolated at zero time which was not possible due to the lack of sensitivity of the method. Non deareated acid solutions are also known to accelerate the corrosion phenomena [26].

The corrosion rates have been also studied as a function of the heat treatment time at 800°C (Figure 4). The protection action is basically the same up to around 15 h. This shows that the film surface coverage of the substrate and probably the structure of the pores are not changed during the heat treatment. There is however a drastic change observed at $t = 20$ h, where the corrosion rates reach the same very high value (CR $\sim$39 MPY) for all systems (higher than that of the as received stainless steel (11.5 MPY at $t = 0$). SEM measurements show that the films are dense with no visible porosity but are completely broken leaving an easy access of the electrolyte to the substrate (Figure 5). The physical reasons of this decohesion is the growth of a layer of Cr_2O_3 single crystals (containing also mainly Mn and Fe) at the interface metal-coating causing significant stresses in the film and leading eventually to its fracture under prolonged high temperature treatment. The growth of the single crystals already occurs at 450°C as confirmed by Rutherford Back Scattering measurements [28].

4. Conclusion

Sol-gel coatings of ZrO_2, SiO_2, $70SiO_2$–$30TiO_2$ and $88SiO_2$–$12Al_2O_3$ compositions have been prepared from sonocatalyzed sols and deposited by dip coating technique of 316L stainless steel foil. All the coatings protect the metallic substrate against acid (15% H_2SO_4) corrosion. The films are shown to act as a geometric blocking layer and increase the lifetime of the substrate by a factor up to 8.5, the effect being more pronounced at 50°C than at room temperature. The electrochemical parameters such as the corrosion potential, polarization resistance and corrosion rate have been determined. These results, together with those already published on the corrosion obtained in NaCl solutions [25] confirm the outstanding corrosion protection behavior of thin sonocatalyzed sol-gel oxide
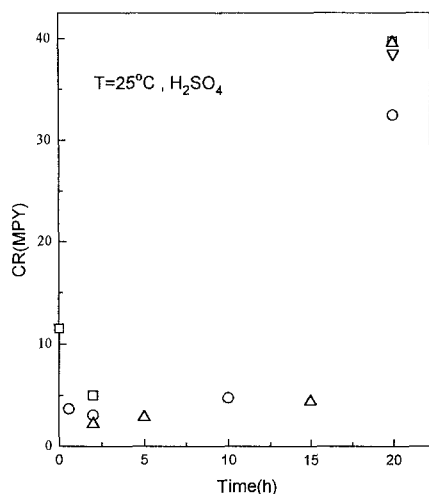
Fig. 4. Corrosion rate (MPY) versus time of heat treatment at 800°C measured at 25°C in 15% H_2SO_4 for (□)ss, (○)SiO_2, (△) SiO_2–TiO_2, ▽ (SiO_2–A l_2O_3).
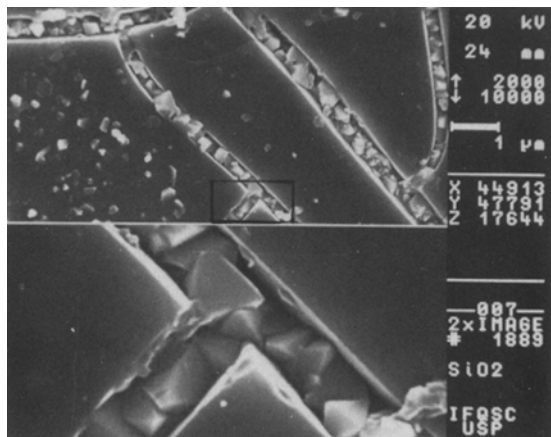

Fig. 5. SEM micrograph of a SiO_2–TiO_2 coating heat treated at 800°C during 20 h showing the fracture of the coating due to the growth of Cr_2O_3 single crystals at the metal/coating interface. The lower part is a 5 times amplification of the inset shown in the micrograph.

films which can be practically used by the chemical and construction industries.

Acknowledgments

References

1. Brinker, C.J. and Scherer, G.W., *Sol-gel Science: the Physics and Chemistry of Sol-gel Processing* (Academic Press, San Diego, 1990).

2. Sakka, S., in *Sol-Gel Science and Technology*, edited by Aegerter, M.A., Jr., M.J., Souza, D.F., Zanotto, E.D., (World Scientific, Singapore, 1991) pp. 346–374.

3. Dislich, H., in *Sol-Gel Technology for Thin Films, Fibers, Preforms, Electronics, and Specialty Shapes*, edited by L.C. Klein (Noyes Publications, Park Ridge, W, 1988) pp. 50–79.

4. Pettit, R.B., Ashley, C.S., Reed, S.T., and Brinker, C.J., in *Sol-gel Technology for Thin Films, Fibers, Preforms, Electronics and Specialty Shapes*, edited by L.C. Klein (Noyes Publications, Park Ridge, 1988) pp. 80–109.

5. Schmidt, H., in *Chemistry, Spectroscopy and Applications of Sol-Gel Glasses*, edited by R. Reisfeld, C.K. Jorgensen (Springer-Verlag, Berlin, 1992) pp. 119–152.

6. Sakka, S. and Yoko, T., in *Chemistry, Spectroscopy and Applications of Sol-Gel Glasses*, edited by R.R., J.C.K. (Springer-Verlag, Berlin, 1992) pp. 89–118.

7. Jones, D.A., *Principles and Prevention of Corrosion* (Maxwell-MacMillan, 1992).

8. Schreir, L.L., *Corrosion* (Newnes-Butterworths, 1976), vol. 2.

9. Schlichting, J., and Neumann, S., J. Non-Cryst. Solids **48** (185), (1982).

10. Martinsen, J., Figat, R.A., and Shafer, M.W., Mat. Res. Soc. Symp. Proc. **32** (361), (1984).

11. Brow, R.K. and Pantano, C.G., Mat. Res. Soc. Symp. Proc. **32** (361), (1982).

12. Ogiwara, S. and Kinugawa, K., Yogyo-Kyokai-Shi (in Japanese) **90** (157), (1982).

13. Matsuda, A., Matsuno, Y., Katagama, S., Tsuno, T., Tohge, N., and Minami, T., J. Ceram. Soc. Jpn., Int. Ed. **100**, 1079–1082 (1992).

14. Sanctis, O., Gomez, L., Pelligri, N., Parodi, C., Marajofsky, A., and Duran, A., J. Non-Cryst. Solids **121** (338), (1990).

15. Tohge, N., Matsuda, A., and Minami, T., J. Am. Ceram. Soc. **70** (C13), (1987).

16. Guglielmi, M., Festa, D., Innocenzi, P.C., Colombo, P., and Gobain, M., J. Non-Cryst. Solids **147–148**, 474–477 (1992).

17. Di Giampaolo, A.R., Puerta, M., Lira, J., and Ruiz, N., J. Non-Cryst. Solids **147–148**, 467–473 (1992).

18. Atik, M. and Aegerter, M.A., J. Non-Cryst. Solids **147–148**, 813–819 (1992).

19. Atik, M. and Zarzycki, J., J. Mat. Sci. Lett. (accepted), (1993).

20. Tomasi, A., Scardi, P., and Marchetti, F., Mat. Res. Soc. Symp. Proc. **271**, 477–483 (1992).

21. Atik, M. and Aegerter, M.A., in *Better Ceramics Through Chemistry V*, edited by Hampden-Smith, M.J., Klemperer, W.G., Brinker, C.J. (MRS, Pittsburgh, 1992), vol. 271, pp. 471–476.

22. Ganguli, D., and Kundu, D., J. Mat. Sci. Lett. **3** (503), (1984).

23. Izumi, K., Tanaka, H., Uchida, Y., Tohge, N., and Minami, T., J. Non-Cryst. Solids **147–148**, 483–487 (1992).

24. Maggio, R.D., Scardi, P., and Tomasi, A., Mat. Res. Soc. Symp. **180** (481), (1990).

25. Lima Neto, P., Atik, M., Avoca, L.A., and Aegerter, M.A., J. Sol-Gel Science and Tech. (accepted), (1993).

26. Uhlig, H.H. and Revie, R.W., *Corrosion and Corrosion Control.* J.W. & Sons, Eds., New York, 1985).

27. Bockriss, J.O., and Reddy, A.K.N., *Modern Electrochemistry* (Plenum Press, 1970), vol. 2.

28. Lima Neto, P., Atik, M., Acquadro, J.C., Avaca, L.A., and Aegerter, M.A., (to be published), (1993).